

# Further analysis of solutions to the time-independent wave packet equations of quantum dynamics. II. Scattering as a continuous function of energy using finite, discrete approximate Hamiltonians

Youhong Huang, Srinivasan S. Iyengar, and Donald J. Kouri

*Department of Chemistry and Department of Physics, University of Houston, Houston, Texas 77204-5641*

David K. Hoffman

*Department of Chemistry and Ames Laboratory, Iowa State University, Ames, Iowa 50011*

(Received 28 September 1995; accepted 11 April 1996)

We consider further how scattering information (the  $S$ -matrix) can be obtained, as a continuous function of energy, by studying wave packet dynamics on a finite grid of restricted size. Solutions are expanded using recursively generated basis functions for calculating Green's functions and the spectral density operator. These basis functions allow one to construct a general solution to both the standard homogeneous Schrödinger's equation and the time-independent wave packet, inhomogeneous Schrödinger equation, in the non-interacting region (away from the boundaries and the interaction region) from which the scattering solution obeying the desired boundary conditions can be constructed. In addition, we derive new expressions for a "remainder or error term," which can hopefully be used to optimize the choice of grid points at which the scattering information is evaluated. Problems with reflections at finite boundaries are dealt with using a Hamiltonian which is damped in the boundary region as was done by Mandelshtam and Taylor [J. Chem. Phys. **103**, 2903 (1995)]. This enables smaller Hamiltonian matrices to be used. The analysis and numerical methods are illustrated by application to collinear  $H+H_2$  reactive scattering. © 1996 American Institute of Physics. [S0021-9606(96)02127-7]

## I. INTRODUCTION

The principal question addressed in this paper is how accurate approximations to continuum scattering states can be constructed using Hamiltonians discretized in finite regions (finite matrix approximations to the true Hamiltonian). The equations<sup>1-5</sup> we choose as our framework for treating this question are provided by the time-independent wave packet Schrödinger equation,

$$(E-H)\xi(E|\alpha k_\alpha n_\alpha) = \frac{i}{2\pi}\chi(0|\alpha n_\alpha), \quad (1)$$

and its formal solution, by the time-independent wave packet Lippmann-Schwinger equation,

$$\xi(E|\alpha k_\alpha n_\alpha) = \frac{i}{2\pi}G(E)\chi(0|\alpha n_\alpha), \quad (2)$$

which constitute new formulations of quantum dynamics. In Eq. (2),  $G(E)$  is an inverse of  $(E-H)$  which satisfies some specific boundary conditions, although not necessarily outgoing wave or causal ones,  $\chi(0|\alpha n_\alpha)$  is a source function which in the original derivations was a wave packet at initial time  $t=0$ ,  $\alpha$  denotes an arrangement channel, and  $k_\alpha$  and  $n_\alpha$  denote the average relative translational momentum and initial internal quantum numbers respectively. The factor  $i/2\pi$  can be absorbed into the definition of the initial source function, if desired. Related methods based on these equations have been used by several other groups recently for scattering calculations.<sup>6,7</sup> When the scattering region in the calculation is taken to be large enough so that the scattering amplitudes can be obtained before the solution is reflected

off the boundary, or an absorbing potential is employed to eliminate boundary reflections, and the initial packet  $\chi(0|\alpha n_\alpha)$  vanishes in the region of the potential, it is easy to prove that, in a restricted region of space discussed below, solutions of Eqs. (1) and (2) can be chosen to be related to the Lippmann-Schwinger (LS) state,  $\Psi_k^+(E)$ , according to,<sup>1-3</sup>

$$\frac{i}{2\pi}G^+(E)\chi(0) = \frac{mA(k)}{\hbar^2k}\Psi_k^+(E), \quad (3)$$

with

$$\Psi_k^+(E) = \psi_k(E) + G^+(E)V\psi_k(E). \quad (4)$$

Here,  $\psi_k(E)$  is the "unperturbed" or "incident" state, and we have chosen to suppress the other quantum labels  $\alpha$  and  $n_\alpha$  for the sake of simplifying the notation (we shall use the more detailed notation when it is necessary to avoid confusion). The region of space in which Eq. (3) is valid is characterized in terms of the packet,  $\chi(0)$ . Because we have assumed that  $\chi(0)$  is nonzero in a finite region *outside* the region where the potential is nonzero, we may speak of the region external to  $\chi(0)$  which is closest (in some well defined sense) to the potential as the "potential side" of the initial wave packet. Then Eq. (3) holds *on the potential side of such an initial wave packet*. Here, also,  $G^+(E)$  is the causal Green's function and  $A(k)$  is the Fourier amplitude of  $\chi(0)$  corresponding to the translational momentum  $\hbar k$ . The foremost advantage of Eqs. (1) and (2) is readily seen from Eq. (3): the causal Lippmann-Schwinger solution, over a range of energies, can be obtained from a single  $\chi(0)$ . In this case, the boundary condition satisfied by the Green's func-

tion  $G^+(E) = (E - H + i\epsilon)^{-1}$  in Eq. (3) is the outgoing scattered wave boundary condition. This boundary condition on the Green's function can be enforced either by introducing a negative imaginary absorbing potential,<sup>10-13</sup> or by explicitly obtaining expansion coefficients,  $a_n^+(E)$ , which reflect the  $+i\epsilon$  in the Green's function, yielding results as a continuous function of the energy  $E$ , and permitting the  $\epsilon \rightarrow 0_+$  limit to be taken.<sup>2</sup> A general, energy-separable Faber polynomial representation of the Green's function,  $G^+(E)$ , valid even when the Hamiltonian is not Hermitian (as occurs when one employs an absorbing potential) also has been developed and applied successfully in solving Eq. (2) for reactive scattering problems over a range of energies.<sup>8,9</sup> However, the differential form of the time-independent wave packet formalism (i.e., Eq. (1)), of course, does not possess specific memory of the boundary conditions associated with its derivation from a time dependent treatment.<sup>5</sup> Thus the equation  $(E - H)\xi = (i/2\pi)\chi(0)$  must be augmented by some specific choice of boundary conditions. In the work of Mandelshtam and Taylor<sup>6</sup> and Jang and Light,<sup>7</sup> initial studies of boundary conditions other than the causal one have been reported. In an earlier paper [4], which we shall call paper I, we have also independently considered more general boundary conditions by combining the solutions  $(i/2\pi)G^+(E)\chi(0)$  and  $(i/2\pi)G^-(E)\chi(0)$  to construct  $\delta(E - H)\chi(0)$ , which is easily seen to yield a continuum solution of the standard time-independent Schrödinger equation. (The operator  $\delta(E - H)$  is the so-called spectral density operator.) In fact, in paper I, a robust procedure for constructing general solutions of the Schrödinger equation was given, since a variety of solutions can, in principle, be obtained from  $\delta(E - H)\chi(0)$  by appropriate choice of  $\chi(0)$ .

When the boundary is moved so close to the interaction region that reflections of the scattered waves occur *before* all the incident waves have experienced scattering by the potential, interferences occur which eventually will produce discrete energy levels, and prevent the extraction of continuous scattering information. In addition to considering boundary conditions other than purely outgoing waves, Mandelshtam and Taylor<sup>6</sup> and Jang and Light<sup>7</sup> also gave alternative procedures for circumventing this difficulty. In the former case, they modified the Chebychev expansion as given by Huang *et al.*<sup>2</sup> by damping the recursion satisfied by the Chebychev polynomials, thereby eliminating problems with boundary reflections. Jang and Light expressed the full Green's function in terms of an eigenfunction expansion in which the eigenfunctions were required to satisfy different boundary conditions than vanishing at the end of the grid. Both techniques required the solution of a system of linear algebraic equations in order to extract the scattering information.

In this paper, we continue to consider our own approach to solutions of Eq. (1) and of the standard homogeneous time-independent Schrödinger equation for a continuous range of energy, satisfying either arbitrary or scattering boundary conditions. We will also consider solutions which are generated on a grid of restricted size. Our treatment makes use of the general final state analysis which we introduced in paper I and we employ a type of damped Hamil-

tonian, rather than damped recursion, to treat boundary reflections. However, our damped Hamiltonian expressions can be directly transformed into the same type of damped recursion expressions that were employed by Mandelshtam and Taylor.<sup>6</sup> We illustrate our approach by an application to the collinear H+H<sub>2</sub> reactive scattering system.

The plan of this paper is as follows. In the next section, we give a detailed analysis for constructing scattering wave functions for a continuous range of energy and extracting scattering information when the system is in a restricted region. This leads to new expressions for the error associated with a particular truncation of the expansion of the solution. In Section III, we give the details of the computational method. Finally, in Section IV we present example calculations and a discussion of the results. Section V contains our conclusions.

## II. ANALYSIS

### A. Chebychev expansions of time-independent and time-dependent states

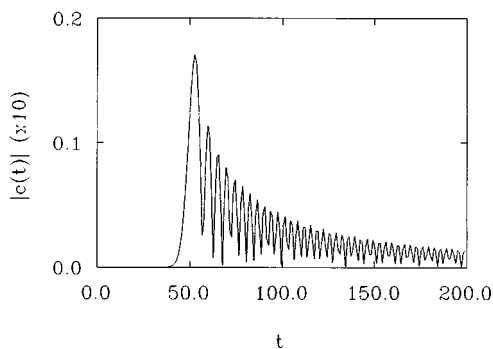
We begin our analysis by considering the polynomial basis set generated by the Faber–Chebychev recursion.<sup>8,9</sup> A time-dependent wave packet  $\chi(t)$  is given in terms of the initial wave packet by

$$\chi(t) = \exp(-itH/\hbar)\chi(0). \quad (5)$$

This equation applies to a general, time-independent Hamiltonian regardless of whether the spectrum is continuous or discrete. If the system is confined to a finite volume (as is usually the case for numerical calculations), then the system Hamiltonian has a totally discrete spectrum. The eigenstates can (more or less cleanly) be divided into two groups depending on whether the boundary conditions are imposed by the spatial extent of the finite region containing the system or by the potential. Those eigenvalues and eigenvectors for which the finite boundaries of the region have a numerically insignificant effect correspond to the bound states of the system in the limit of an infinite volume, whereas the states that have boundary conditions imposed by the finite volume correspond to the continuum for the infinite-volume problem.

For a physical scattering problem for which conservation of energy applies, in the energy range of interest, the Hamiltonian can be represented to arbitrary accuracy on a discrete grid of finite extent by controlling the system volume and the grid spacing. Our objective is to do this as efficiently as possible for numerical calculations. Of course, such a finite grid can only represent a finite number of states. The highly oscillatory, highly energetic eigenvectors that are assumed to contribute little to the wave packet as it evolves are totally ignored, and in some manner or another we must in effect “interpolate” on the discrete states corresponding to the continuum of the infinite-volume system to deduce accurate approximations to these true continuum states. We now turn our attention to how this can be done.

The grid representation of the Hamiltonian (grid Hamiltonian) for a spatially confined system has a finite number of eigenvalues and hence a maximum and a minimum eigen-

FIG. 1.  $|c_n(t)|$  vs  $t$ .  $n=50$  and  $\Delta H/\hbar=1$ .

value. Therefore, the operator  $\exp(-itH/\hbar)$  can be expanded in a Faber–Chebyshev series according to<sup>10,11</sup>

$$\exp(-itH/\hbar) = \sum_{n=0}^{\infty} a_n(t) T_n(H_{\text{norm}}), \quad (6)$$

where

$$a_n(t) = (2 - \delta_{n0})(-i)^n \exp(-it\bar{H}/\hbar) J_n(\Delta H t/\hbar). \quad (7)$$

Here  $\bar{H}$  is the estimated midpoint of the spectrum of  $H$ ,  $\Delta H$  is the estimated half-width of the spectrum, and  $J_n$  is a cylinder Bessel function of the first kind (of integral order). Using the orthogonality relationship for Bessel functions of the same argument but different orders,<sup>12</sup> we can invert this relationship to obtain

$$T_n(H_{\text{norm}}) = \int_{-\infty}^{\infty} dt c_n(t) \exp(-itH/\hbar), \quad (8)$$

where

$$c_n(t) = \sqrt{2n} [(2 - \delta_{n0})(-i)^n \times \exp(-it\bar{H}/\hbar)]^{-1} |t|^{-1} J_n(\Delta H t/\hbar) \quad (9)$$

and  $c_0(t) = \lim_{n \rightarrow 0} c_n(t)$ . The behavior of  $|c_n(t)|$  as a function of  $|t|$  is shown in Fig. 1.

The wave packet  $\chi(t)$ , which evolves from  $\chi(0)$  according to Eqs. (5) and (6), is given by

$$\chi(t) = \sum_{n=0}^{\infty} a_n(t) \eta_n, \quad (10)$$

where

$$\eta_n = T_n(H_{\text{norm}}) \chi(0) \quad (11)$$

is the  $n$ th Faber–Chebyshev vector in the basis set ( $\eta_n$ ;  $n=0$  to  $\infty$ ). From Eq. (8) we have that

$$\eta_n = \int_{-\infty}^{\infty} dt c_n(t) \chi(t). \quad (12)$$

It is apparent from Fig. 1 that these vectors form a kind of “chronological” basis set in that  $\eta_n$  is formed as a transform of  $\chi(t)$  over two time periods (one for positive  $t$  and one for negative  $t$ ). The onset of these time periods grows more or less linearly with  $n$ , and hence  $n$  serves as a rough measure

of  $|t|$ . This onset is relatively sharp; however, packets evolved longer than the onset time continue to contribute with decreasing amplitude. The time interval for a given  $\eta_n$  is somewhat shorter than indicated by Fig. 1 because  $c_n(t)$  is oscillatory and some cancellation due to the phase takes place in the integral of Eq. (12). Thus, we find that an expansion of a function in terms of Faber–Chebyshev basis functions,  $\eta_n$ , is in effect an expansion in terms of (overlapping) periods in the time evolution of the initial wave packet.

## B. Expansion of solutions of the standard homogeneous time-independent Schrödinger equation

We now explore the construction of approximate eigenvectors of  $H$  in terms of a finite linear combination of the Faber–Chebyshev basis functions. To this end, we define

$$\psi_m(E) = \sum_{n=0}^m b_n(E) \eta_n, \quad (13)$$

where the coefficients  $b_n(E)$  are functions, yet to be determined, of an arbitrarily chosen energy. We seek to choose the coefficients in such a way that, to a controllable approximation,

$$H \psi_m(E) \approx E \psi_m(E). \quad (14)$$

By definition

$$H = (\Delta H) H_{\text{norm}} + \bar{H} \quad (15)$$

and thus

$$H \psi_m(E) = \bar{H} \psi_m(E) + \Delta H \left[ b_0 H_{\text{norm}} + \sum_{n=1}^m b_n H_{\text{norm}} T_n(H_{\text{norm}}) \right] \chi(0), \quad (16)$$

where we have made use of the fact that  $T_0=1$ . The recursion relation for the Chebyshev polynomials is

$$x T_n(x) = \frac{1}{2} [T_{n+1}(x) + T_{n-1}(x)], \quad n \geq 1 \quad (17)$$

which when substituted in Eq. (16) yields

$$H \psi_m(E) = \bar{H} \psi_m(E) + \Delta H \left[ b_0 H_{\text{norm}} + b_1/2 + (b_2/2) H_{\text{norm}} + T_m(H_{\text{norm}}) b_{m-1}/2 + T_{m+1}(H_{\text{norm}}) b_m/2 + \frac{1}{2} \sum_{n=2}^{m-1} (b_{n-1} + b_{n+1}) T_n(H_{\text{norm}}) \right] \chi(0). \quad (18)$$

If we now define  $b_0=1/2$  and  $b_n(E) = T_n(E_{\text{norm}})$  for  $n \geq 1$  where  $E_{\text{norm}} = (E - \bar{H})/\Delta H$  we then have from Eq. (17) that

$$b_0 H_{\text{norm}} + \frac{1}{2} b_2 H_{\text{norm}} = E_{\text{norm}} b_1 H_{\text{norm}} \quad (19)$$

and

$$\frac{1}{2} [b_{n-1} + b_{n+1}] T_n(H_{\text{norm}}) = E_{\text{norm}} b_n T_n(H_{\text{norm}}), \quad (20)$$

and thus

$$H\psi_m(E) = E\psi_m(E) + \widetilde{R}_m(E), \quad (21)$$

where the remainder function,  $\widetilde{R}_m(E)$ , is defined by

$$\widetilde{R}_m(E) \equiv (\Delta H/2)[T_m(E_{\text{norm}})\eta_{m+1} - T_{m+1}(E_{\text{norm}})\eta_m]. \quad (22)$$

This expression is similar in structure to the Christoffel–Darboux formula<sup>12</sup> associated with sums of orthogonal polynomials. It is apparent that for those regions in the confining volume where  $\widetilde{R}_m(E)$  is very small,  $\psi_m(E)$  is an approximate eigenfunction of  $H$ , but, of course, not necessarily one that obeys the boundary conditions imposed by the constraints of finite volume. The latter is not a problem since in most cases the size of the finite region is employed solely for numerical convenience and does not impose boundary conditions of physical interest. If the energy-independent  $\eta_m$  and  $\eta_{m+1}$  are both separately small then  $\psi_m(E)$  provides an approximate eigenfunction for any energy, which is a point we later discuss in more detail.

We now examine the convergence of the infinite series,

$$\begin{aligned} \widetilde{\psi}(E) &= \lim_{m \rightarrow \infty} \psi_m(E) \\ &= \left[ 1/2 + \sum_{n=1}^{\infty} T_n(E_{\text{norm}})T_n(H_{\text{norm}}) \right] \chi(0). \end{aligned} \quad (23)$$

From the completeness relation for Chebychev polynomials we have that

$$\omega(E_{\text{norm}})\widetilde{\psi}(E)/(\pi\Delta H) = \delta(E-H)\chi(0), \quad (24)$$

where  $\omega(E_{\text{norm}}) = (1 - E_{\text{norm}}^2)^{-1/2}$  is the weight function for orthogonality of the Chebychev polynomials. As has been discussed in paper I,<sup>4</sup> Eq. (24) obviously provides a formal solution to the standard homogeneous time-independent Schrödinger equation. However, the initial wave packet can always be expanded in terms of the spectrum of  $H$  according to

$$|\chi(0)\rangle = \sum_{\sigma} |\sigma\rangle \langle \sigma | \chi(0)\rangle, \quad (25)$$

where  $\{\sigma\}$  is a complete set of quantum numbers (which are discrete, and in fact finite, because  $H$  is the grid representation of the Hamiltonian for a spatially confined system), and from this equation it is clear that  $\delta(E-H)\chi(0)$  is either zero or infinite as a function of  $E$  and hence that Eq. (24) is only a solution to the Schrödinger equation in a formal sense. Two points should be made here.

(1) In our numerical approach we deal only with Hamiltonians that have a finite spectrum because we reduce the Hamiltonian to a matrix of finite dimensions. However, in the continuum of the Hamiltonian for a true scattering system,  $\delta(E-H)\chi(0)$  is a scattering (i.e., improper) eigenfunction.<sup>4</sup>

(2) Even though  $\delta(E-H)\chi(0)$  does not converge for an operator with a discrete spectrum, with appropriate generalization, it still provides the conceptual framework for a very efficient diagonalization procedure for such matrices.<sup>13,14</sup>

### C. Expansion of solutions of the inhomogeneous time-independent wave packet Schrödinger and Lippmann–Schwinger equations

The above analysis can be utilized also for generating solutions of the inhomogeneous time-independent wave packet Schrödinger equation, rather than Eq. (14). Thus, we consider the equation

$$H\xi_m(E) = E\xi_m(E) - \frac{i}{2\pi}\chi(0), \quad (26)$$

and note that the general solution will be a combination of the homogeneous solution (already discussed above), plus a particular solution of the inhomogeneous equation. We can develop the desired general solution as

$$\xi_m(E) = \sum_{n=0}^m g_n(E)\eta_n, \quad (27)$$

in analogy with Eq. (10) for the homogeneous solution. In fact, the  $g_n(E)$  will be complex, with the real part being equal, to within a constant, to the  $b_n$  already discussed:

$$\text{Re}[g_n(E)] = \pm \frac{\omega(E_{\text{norm}})}{2\pi\Delta H} b_n(E), \quad \text{all } n. \quad (28)$$

Note that this relationship between  $\text{Re}[g_n(E)]$  and the  $b_n(E)$  corresponds to a change in the normalization of the solution,  $\psi(E)$ , of the homogeneous Schrödinger equation (compared to  $\widetilde{\psi}(E)$ ) which is imposed simply because the particular solution's normalization is not arbitrary; it must be such as to generate the correct normalization of the inhomogeneity  $i\chi(0)/2\pi$ . The sign choice determines whether one is generating a causal-like or anticausal-like solution of the inhomogeneous equation, since

$$\xi^{\pm}(E) = \frac{i}{2\pi} G^{\pm}(E)\chi(0), \quad (29)$$

$$= \frac{i}{2\pi} G^P(E)\chi(0) \pm \frac{1}{2} \delta(E-H)\chi(0). \quad (30)$$

Then

$$\xi^{\pm}(E) = \pm \frac{1}{2} \psi(E) + \frac{i}{2\pi} G^P(E)\chi(0) \quad (31)$$

$$= \pm \xi^R + i\xi^I(E). \quad (32)$$

As stated above,  $\psi(E)$  is related to  $\widetilde{\psi}(E)$  according to

$$\psi(E) = \omega(E_{\text{norm}})\widetilde{\psi}(E)/(\pi\Delta H). \quad (33)$$

We next follow the same procedure as before, substituting Eq. (27) into Eq. (26), to obtain

$$\begin{aligned} H\xi_m(E) &= \overline{H}\xi_m(E) + \Delta H \left[ g_0 H_{\text{norm}} \right. \\ &\quad \left. + \sum_{n=1}^m g_n H_{\text{norm}} T_n(H_{\text{norm}}) \right] \chi(0). \end{aligned} \quad (34)$$

The choice Eq. (28) will ensure that the real part of  $g_n$ , combined with the recursion Eq. (14), leads to

$$H\xi_m^R(E) = E\xi_m^R + R_m^H/2 \tag{35}$$

and the imaginary part of  $g_n$  leads to

$$H\xi_m^I(E) = \bar{H}\xi_m^I(E) + \Delta H \left[ g_0^I H_{\text{norm}} + \frac{1}{2} \{g_1^I + g_2^I H_{\text{norm}} + g_{m-1}^I T_m(H_{\text{norm}}) + g_m^I T_{m+1}(H_{\text{norm}})\} \chi(0) + \frac{\Delta H}{2} \left[ \sum_{n=2}^{m-1} (g_{n-1}^I + g_{n+1}^I) T_n(H_{\text{norm}}) \right] \chi(0) \right] \tag{36}$$

We have attached the superscript ‘‘H’’ to  $R_m$ , given by Eq. (19), to indicate that it is the remainder term for the solution of the *homogeneous* equation. Again,  $R_m^H$  is related to  $\tilde{R}_m(E)$  by a relation similar to that between  $\psi(E)$  and  $\tilde{\psi}(E)$ .

We now note that one may introduce the linearly independent Chebychev functions,  $V_n(E_{\text{norm}})$ ,

$$V_n(E_{\text{norm}}) = \sin(n\varphi(E)), \tag{37}$$

which also satisfy the recursion<sup>15</sup>

$$xV_n(x) = \frac{1}{2}[V_{n+1}(x) + V_{n-1}(x)]. \tag{38}$$

The phase  $\varphi(E)$  equals  $\cos^{-1}E_{\text{norm}}$ . We then choose

$$g_0^I(E) = 0, \tag{39}$$

$$g_1^I(E) = -\frac{1}{\pi\Delta H} \tag{40}$$

$$\equiv -\frac{\omega(E_{\text{norm}})}{\pi\Delta H} V_1(E_{\text{norm}}), \tag{41}$$

and

$$g_n^I(E) = -\frac{\omega(E_{\text{norm}})}{\pi\Delta H} V_n(E_{\text{norm}}), \quad n \geq 1. \tag{42}$$

Since

$$V_0(E_{\text{norm}}) \equiv 0, \tag{43}$$

it is easy to verify that

$$E_{\text{norm}}V_1(E_{\text{norm}}) = \frac{1}{2}V_2(E_{\text{norm}}), \tag{44}$$

and using these equations, and the recursion (38), in Eq. (36) yields the final result

$$H\xi_m^I(E) = E\xi_m^I(E) - \frac{1}{2\pi}\chi(0) + R_m^I(E). \tag{45}$$

It should be noted that the above choices of real and imaginary parts of  $g_n(E)$  correspond to

$$g_n(E_{\text{norm}}) = -\frac{\omega(E_{\text{norm}})}{\pi\Delta H} [\cos(n\varphi(E)) - i\sin(n\varphi(E))] = -\frac{\omega(E_{\text{norm}})}{\pi\Delta H} e^{-in\varphi(E)}. \tag{46}$$

Here, the energy-dependent phase,  $\varphi(E)$ , is

$$\varphi(E) = \cos^{-1}\left(\frac{E - \bar{H}}{\Delta H}\right), \tag{47}$$

and  $\bar{H}$  and  $\Delta H$  are the center and the half width of the spectrum of the Hermitian Hamiltonian,  $H$ , respectively. The remainder,  $R_m^I(E)$ , for the particular solution of Eq. (1) is

$$R_m^I(E) = -\frac{\omega(E_{\text{norm}})}{2\pi} [V_m(E_{\text{norm}})\eta_{m+1} - V_{m+1}(E_{\text{norm}})\eta_m]. \tag{48}$$

In this expression,  $\xi_m^I(E)$  is now expressed explicitly as

$$\xi_m^I(E) = -\frac{\omega(E_{\text{norm}})}{\pi\Delta H} \sum_{n=1}^m V_n(E_{\text{norm}})T_n(H_{\text{norm}})\chi(0) \tag{49}$$

$$\equiv -\frac{\omega(E_{\text{norm}})}{\pi\Delta H} \sum_{n=0}^m V_n(E_{\text{norm}})T_n(H_{\text{norm}})\chi(0), \tag{50}$$

where the latter makes use of the fact that  $V_0$  vanishes. We note that in previous work we have shown that<sup>11,17</sup>

$$\lim_{m \rightarrow \infty} \sum_{n=0}^m V_n(E_{\text{norm}})T_n(H_{\text{norm}})\chi(0) = -\frac{\sqrt{(\Delta H)^2 - (E - \bar{H})^2}}{2} G^P(E)\chi(0). \tag{51}$$

Thus, this procedure is a general one that makes possible the generation of both the solution of the homogeneous time-independent Schrödinger equation and the particular solution of the inhomogeneous time-independent Schrödinger equation, for *any* energy  $E$ . We emphasize that the energy  $E$  can be varied continuously, so that the solutions thus constructed are true scattering-type states, as will now be discussed.

### D. Extraction of scattering information as a continuous function of energy and the role of the ‘‘box-size’’

We now examine how functions satisfying Eq. (21) can be used to extract scattering information. The first case we consider is that of a packet, initially in a precollision region, impinging on a target. We further assume that the grid is very long so that the collision, to the desired numerical accuracy, has been completed before any portion of the packet traverses the finite scattering region. The time-to-energy transform of  $\chi(t)$ ,

$$\int_{-\infty}^{\infty} dt \exp(iEt/\hbar)\chi(t) \tag{52}$$

provides a scattering eigenfunction of the system with a causal boundary condition if  $E$  is in the continuum. If we consider a particular position of the system in configuration space, then the integral at this configuration has effectively converged once the packet has passed over this configuration point and exited the system. (Some care must be exercised here because, due to wave packet spreading, the wave packet actually never totally leaves any region of space. In fact, in one and two dimensions the integral, Eq. (52), is not abso-

lutely convergent<sup>18</sup> and convergence of the integral relies to an extent on phase oscillations. This is the reason for the use of the term “effectively.” In higher dimensions, where the wave spreads in time in a configuration space of greater dimensionality, the integral does converge absolutely.<sup>18</sup> Suppose  $t_m$  is the onset time for the Faber–Chebychev basis function  $\eta_m$ . Then, if for times such that  $|t| > |t_m|$ , the packet has effectively passed over the configuration point, the Christoffel–Darboux remainder term of Eq. (22) vanishes and  $\psi_m(E)$  satisfies the time-independent Schrödinger equation for *any scattering energy* ( $E$ ). This solution is obviously not an eigenfunction of the grid Hamiltonian used to construct Eq. (22) since it does not satisfy the boundary conditions imposed by the finite volume. Instead it is a true scattering solution, assuming as we have that the packet has not reached the boundary of the finite region and been reflected back. However, for large  $m$ ,  $\eta_m$  will not vanish because the wave packet for the grid Hamiltonian will reflect off the boundary and scatter back across the configuration point, and, as we have discussed, in the limit as  $m$  becomes infinite  $\psi_m(E)$  does not converge. Thus, in this circumstance,  $\psi_m(E)$  converges *asymptotically* as a function of  $m$  to the true scattering wave function for the Hamiltonian without finite boundaries. Similar results hold for the particular solution of the inhomogeneous time-independent Schrödinger equation.

If the initial wave packet is not “precollision” but instead starts out overlapping the scattering region, then  $\psi_m(E)$  still converges asymptotically to a scattering eigenfunction at a configuration point if the packet has not reflected off the walls so that the Christoffel–Darboux remainder vanishes. However, the construction of a scattering solution with the desired boundary conditions, in general, will require the use of more than one initial packet.<sup>4</sup> (Note that we do *not* seek solutions of the inhomogeneous time-independent wave packet Schrödinger equation when  $\chi(0)$  overlaps the scattering region.)

Obtaining asymptotic convergence in Eq. (21) or Eq. (45) requires a grid sufficiently large so that the  $\eta_n$  vectors in the expansion do not reflect off the boundaries of the finite scattering region before the collision of interest is completed. This often times requires a very large grid. A well established procedure for shortening the required grid size is to use an imaginary absorbing potential at the boundaries of the scattering region.<sup>16,17,19,20</sup> In this case the  $\eta_n$  are absorbed rather than reflected off the boundaries of the grid. However, adding an imaginary potential to the Hamiltonian gives it a complex spectrum, which alters the radius of the convergence of the Chebychev polynomial expansion, and thus the definition of  $H_{\text{norm}}$  must be adjusted accordingly<sup>8,9</sup> (to keep the Christoffel–Darboux remainder from diverging). From a numerical point of view using a non-Hermitian Hamiltonian is substantially less convenient than using a Hermitian one. One procedure given recently by Mandelshtam and Taylor is to employ (effectively) an energy-dependent absorbing potential.<sup>6</sup> However, they show that by appropriate modification of the Chebychev recursion relation it is still possible to deal with the physical Hamiltonian. The effect of the ab-

sorbing potential is to include exponential damping in the recursion relation.

### E. Eliminating boundary reflections using “Mandelshtam–Taylor-type” damping

We now examine a method for extracting scattering information using a Hermitian grid Hamiltonian by modifying the Faber–Chebychev recursion relation of Eq. (17). Let us consider the “damped grid Hamiltonian”<sup>6</sup>

$$H_{\text{damp}}(x_l, x_{l'}) = \sqrt{d(x_l)} H_{\text{norm}}(x_l, x_{l'}) \sqrt{d(x_{l'})}, \quad (53)$$

where  $d(x_l)$  and  $d(x_{l'})$  can be viewed as elements of a diagonal, real matrix, and  $x_l$  denotes grid points in the configuration space of the collision system. Furthermore, we assume the function  $d$  to be a “damping function” which is equal to unity at grid points in the interior of the scattering region but whose values decay smoothly to zero at grid points in the boundary regions. We then use the  $d(x_l)$  to modify or “scale” the Faber–Chebychev recursion relations for the  $\eta_n$ , defining

$$\eta_0^d(x_l) = \chi(0|x_l), \quad (54)$$

$$\eta_1^d(x_l) = \sum_{l'} H_{\text{damp}}(x_l, x_{l'}) \chi(0|x_{l'})$$

and

$$\eta_{n+1}^d(x_l) = 2 \sum_{l'} H_{\text{damp}}(x_l, x_{l'}) \eta_n^d(x_{l'}) - d^2(x_l) \eta_{n-1}^d(x_l), \quad n \geq 1. \quad (55)$$

Making use of these *modified Faber–Chebychev recursion relations*, Eq. (18) assumes the form

$$\begin{aligned} H\psi_m(E) = & \bar{H}\psi_m(E) + \Delta H[b_0 H_{\text{damp}}] \eta_0^d + (b_1/2) d^2 \eta_0^d \\ & + (b_2/2) d^2 \eta_1^d + (b_{m-1}/2) \eta_m^d + (b_m/2) \eta_{m+1}^d \\ & + \frac{1}{2} \sum_{n=2}^{m-1} [b_{n-1} + d^2 b_{n+1}] \eta_n^d \end{aligned} \quad (56)$$

or

$$\begin{aligned} H\psi_m(E) = & E\psi_m(E) + \tilde{R}_m(E) \\ & + \frac{1}{2} (d^2 - 1) \sum_{n=0}^{m-1} T_{n+1}(E_{\text{norm}}) \eta_n^d. \end{aligned} \quad (57)$$

In this equation,  $H$  and  $H_{\text{damp}}$  are the grid Hamiltonian and damped grid Hamiltonian matrices,  $d^2$  is a diagonal matrix with elements  $\delta_{ll'} d^2(x_l)$ , and the  $\psi_m(E)$ ,  $\tilde{R}_m(E)$ , and  $\eta_n$  are discrete vectors. To obtain the final form of the result, we have taken  $b_0 = 1/2$  and  $b_n = T_n(E_{\text{norm}})$  for  $n \geq 1$  as before. An analogous result holds for the particular solution of Eq. (1).

We first remark that the modified Faber–Chebychev basis vectors are *not* derived by applying Chebychev polynomials of the damped Hamiltonian to a trial vector (cf. Eq. (11)) as is obvious from the fact that Eq. (55) is not the same recursion relation as Eq. (17). However, in the interior region

where  $d^2=1$ , Eq. (55) locally becomes equivalent to Eq. (17). As a result  $\eta_m$  propagates in  $m$  in the same manner as  $T_m(H_{\text{norm}})\chi(0)$ , until it reaches the boundary region. There, the damping factor in the recursion attenuates the reflected wave so that in the limit

$$\lim_{m \rightarrow \infty} \eta_m^d = 0 \quad (58)$$

and as a result

$$\lim_{m \rightarrow \infty} \tilde{R}_m = 0. \quad (59)$$

Thus, Eq. (57) becomes

$$H\tilde{\psi}(E) = E\tilde{\psi}(E) + \frac{1}{2}(d^2-1) \sum_{n=0}^{\infty} T_{n+1}(E_{\text{norm}}) \eta_n^d, \quad (60)$$

where  $\tilde{\psi}(E) \equiv \lim_{m \rightarrow \infty} \psi_m(E)$ . It follows that, in the interior region,  $(d^2-1)$  can be made sufficiently small that  $\tilde{\psi}(E)$  obeys the time-independent (homogeneous) Schrödinger equation for arbitrary  $E$ . If the reflected basis vectors are completely attenuated so that they never return to the region where the scattering analysis is carried out, then  $\tilde{\psi}(E)$  obeys causal boundary conditions, and one can use the simple analysis based on Eq. (1) (provided that  $\chi(0)$  does not overlap the potential). However, if the reflected basis vectors do reach the analysis region as  $m$  increases, then  $\tilde{\psi}(E)$  does not satisfy any special boundary condition. In this case, one must use a complete set of linearly independent initial packets to construct a wave function that satisfies the desired boundary conditions. It should be clear that the parallel development can be given for  $\xi_m^I$ , the particular solution of Eq. (1), and for the homogeneous solution  $\psi(E)$ , with remainder  $R_m^H(E)$ .

## F. One-dimensional illustration

We now consider a one-dimensional problem to illustrate the analysis. Suppose the initial wave packet,  $\chi(0)$ , is located on the LHS of the potential (without overlapping it) and is impinging on the target. The general solution of the time-independent Schrödinger equation with arbitrary boundary conditions is given by a linear combination of any complete set of linearly independent solutions. These can be chosen in a number of ways, for example as the real and imaginary parts of a complex solution (assuming a real Hamiltonian). One particular choice of general solution is

$$\Psi(E|x) = a\Psi_k^+(E|x) + b\Psi_{-k}^+(E|x), \quad (61)$$

where  $\Psi_{\pm k}^+$ ,  $k>0$  are the linearly independent causal solutions of the Lippmann–Schwinger (LS) equations corresponding to scattering waves propagating in the  $\pm x$  direction with energy  $E = \hbar^2 k^2/2m$ . Outside and to the left of the potential we have that

$$\Psi_k^+(E|x) = \exp(ikx) + R \exp(-ikx) \quad (62)$$

and

$$\Psi_{-k}^+(E|x) = T' \exp(-ikx) \quad (63)$$

and to the right of the potential

$$\Psi_k^+(E|x) = T \exp(ikx) \quad (64)$$

and

$$\Psi_{-k}^+(E|x) = \exp(-ikx) + R' \exp(ikx). \quad (65)$$

Here  $R$  (and  $R'$ ) and  $T$  (and  $T'$ ) are, respectively, the energy dependent reflection and transmission amplitudes. (The primed and unprimed quantities differ at most by a phase.) These amplitudes and the constant coefficients  $a$  and  $b$  can be obtained by evaluating  $\Psi(E|x)$  at two points in the region between  $\chi(0)$  and the beginning of the potential and at two points beyond and to the right of the potential.<sup>4</sup>

## G. Final state analysis for reactive scattering

The same analysis can be generalized readily for reactive scattering. In the case of two arrangements,  $\alpha$  and  $\beta$ , an arbitrary solution of the time-independent Schrödinger equation can be written as a linear combination of the causal LS solutions,  $\Psi_{\lambda_\alpha}^+(E|\alpha)$  and  $\Psi_{\lambda_\beta}^+(E|\beta)$ . Here the subscripts  $\lambda_\alpha$  and  $\lambda_\beta$  fix the solution by specifying the precollision states in the  $\alpha$  and  $\beta$  arrangement channels, respectively. The asymptotic forms of  $\Psi_{\lambda_\alpha}^+(E|\alpha)$  and  $\Psi_{\lambda_\beta}^+(E|\beta)$  are given by

$$\begin{aligned} \Psi_{\lambda_\alpha}^+(E|\alpha|\vec{x}) &= \psi_{\lambda_\alpha}^-(E|\alpha|\vec{x}) \\ &+ \sum_{\lambda'_\alpha=1}^{N_\alpha(E)} \sqrt{\frac{k_{\lambda_\alpha}}{k_{\lambda'_\alpha}}} S_{\lambda_\alpha \lambda'_\alpha}(E) \psi_{\lambda'_\alpha}^+(E|\alpha|\vec{x}), \end{aligned} \quad (66)$$

$$\Psi_{\lambda_\beta}^+(E|\beta|\vec{x}) = \sum_{\lambda'_\beta=1}^{N_\beta(E)} \sqrt{\frac{k_{\lambda_\beta}}{k_{\lambda'_\beta}}} S_{\lambda_\beta \lambda'_\beta}(E) \psi_{\lambda'_\beta}^+(E|\beta|\vec{x}),$$

valid outside the potential on the  $\alpha$  arrangement side, and

$$\Psi_{\lambda_\alpha}^+(E|\alpha|\vec{x}) = \sum_{\lambda'_\beta=1+N_\alpha(E)}^{N_\beta(E)+N_\alpha(E)} \sqrt{\frac{k_{\lambda_\alpha}}{k_{\lambda'_\beta}}} S_{\lambda_\alpha \lambda'_\beta}(E) \psi_{\lambda'_\beta}^+(E|\beta|\vec{x}),$$

$$\begin{aligned} \Psi_{\lambda_\beta}^+(E|\beta|\vec{x}) &= \psi_{\lambda_\beta}^-(E|\beta|\vec{x}) \\ &+ \sum_{\lambda'_\beta=1+N_\alpha(E)}^{N_\beta(E)+N_\alpha(E)} \sqrt{\frac{k_{\lambda_\beta}}{k_{\lambda'_\beta}}} S_{\lambda_\beta \lambda'_\beta}(E) \psi_{\lambda'_\beta}^+(E|\beta|\vec{x}), \end{aligned} \quad (67)$$

valid outside the potential on the  $\beta$  arrangement side.  $\psi_{\lambda_\alpha}^\pm(E)$  are the *unperturbed* channel functions (consisting of a product of an internal state and a traveling wave in the appropriate Jacobi translational variable).  $N_{\alpha(\beta)}(E)$  is the number of open channels in the  $\alpha(\beta)$  arrangement. We use a notation convention commonly employed in calculations, where the coefficients in the superposition of the linearly independent unperturbed channel functions are indexed sequentially from 1 up to  $N_\alpha + N_\beta$ . Thus, e.g., a symmetric reaction involves twice the number of channels as are open in one arrangement, and the  $A$  and  $B$  matrices have indices that range from 1 to  $2N_\alpha$ . In Eq. (61) (and equations that

follow) the  $\beta$ -arrangement channels *start* at  $N_\alpha + 1$  and extend up to  $N_\alpha + N_\beta$ , which for a symmetric reaction equals  $2N_\alpha$ .

Combining Eqs. (66) and (67), one obtains

$$\begin{aligned} \xi_i(E|\vec{x}) &= \sum_{\lambda_\alpha=1}^{N_\alpha(E)} A_{i\lambda_\alpha} \psi_{\lambda_\alpha}^-(E|\alpha|\vec{x}) \\ &+ \sum_{\lambda_\alpha=1}^{N_\alpha(E)} B_{i\lambda_\alpha} \psi_{\lambda_\alpha}^+(E|\alpha|\vec{x}) \end{aligned} \quad (68)$$

just outside the potential in the  $\alpha$  arrangement, and

$$\begin{aligned} \xi_i(E|\vec{x}) &= \sum_{\lambda_\beta=1+N_\alpha(E)}^{N_\beta(E)+N_\alpha(E)} A_{i\lambda_\beta} \psi_{\lambda_\beta}^-(E|\beta|\vec{x}) \\ &+ \sum_{\lambda_\beta=1+N_\alpha(E)}^{N_\beta(E)+N_\alpha(E)} B_{i\lambda_\beta} \psi_{\lambda_\beta}^+(E|\beta|\vec{x}) \end{aligned} \quad (69)$$

just outside the potential in the  $\beta$  arrangement. The matrix elements of  $B$  are defined by<sup>4</sup>

$$\begin{aligned} B_{i\lambda_\alpha} &= \sum_{\lambda'_\alpha=1}^{N_\alpha(E)} \sqrt{\frac{k_{\lambda'_\alpha}}{k_{\lambda_\alpha}}} A_{i\lambda'_\alpha} S_{\lambda'_\alpha\lambda_\alpha}(E) \\ &+ \sum_{\lambda'_\beta=1+N_\alpha(E)}^{N_\beta(E)+N_\alpha(E)} \sqrt{\frac{k_{\lambda'_\beta}}{k_{\lambda_\alpha}}} A_{i\lambda'_\beta} S_{\lambda'_\beta\lambda_\alpha}(E), \\ B_{i\lambda_\beta} &= \sum_{\lambda'_\alpha=1}^{N_\alpha(E)} \sqrt{\frac{k_{\lambda'_\alpha}}{k_{\lambda_\beta}}} A_{i\lambda'_\alpha} S_{\lambda'_\alpha\lambda_\beta}(E) \\ &+ \sum_{\lambda'_\beta=1+N_\alpha(E)}^{N_\beta(E)+N_\alpha(E)} \sqrt{\frac{k_{\lambda'_\beta}}{k_{\lambda_\beta}}} A_{i\lambda'_\beta} S_{\lambda'_\beta\lambda_\beta}(E) \end{aligned} \quad (70)$$

for  $i = 1, 2, \dots, N_\alpha(E) + N_\beta(E)$ . Equation (70) can be written in a matrix form

$$\tilde{B} = \tilde{A}S, \quad (71)$$

where

$$\begin{aligned} \tilde{A}_{ij} &= \sqrt{k_j} A_{ij}, \\ \tilde{B}_{ij} &= \sqrt{k_j} B_{ij}. \end{aligned} \quad (72)$$

Equations (68) and (69) can be interpreted as two coupled linear algebraic equations for the matrices  $A$  and  $B$ , which can be found by several methods. Using the method in paper I,<sup>4</sup> one obtains the  $2(N_\alpha(E) + N_\beta(E)) \times (N_\alpha(E) + N_\beta(E))$  matrix elements of  $A$  and  $B$  by evaluating the solution  $\xi(E|\vec{x})$  at  $2N_\alpha(E)$  points in the  $\alpha$  arrangement and  $2N_\beta(E)$  points in the  $\beta$  arrangement for each of the initial, linearly independent wave packets,  $\chi_i(0), i = 1, 2, \dots, (N_\alpha(E) + N_\beta(E))$ . The full  $S$ -matrix can be obtained by solving Eq. (71) together with Eq. (72), i.e.,

$$S = \tilde{A}^{-1} \tilde{B}. \quad (73)$$

It should be noted that one *can* reduce the number of packets that must be propagated by taking advantage of the fact that

the solutions generated are complex. It is well known that the real and imaginary parts of a complex solution of the homogeneous TISE are separate solutions. This has been discussed in detail for simple 1D potential scattering in paper I, and similar techniques can be used for reactive scattering.

The matrices  $A$  and  $B$  can also be obtained using appropriate final wave packets, or ‘‘test functions,’’  $|\chi_f\rangle$  (again, see paper I). Constructing a final wave packet with a specific channel in an arrangement,  $\langle \chi_f(\alpha(\beta)|\lambda_{\alpha(\beta)})|$ , and projecting the solution  $|\xi(E)\rangle$  onto the final wave packet, one gets

$$\begin{aligned} \langle \chi_f(\alpha|\lambda_\alpha)|\xi(E)\rangle &= A_{i\lambda_\alpha} \langle \chi_f(\alpha|\lambda_\alpha)|\psi_{\lambda_\alpha}^-(E|\alpha)\rangle \\ &+ B_{i\lambda_\alpha} \langle \chi_f(\alpha|\lambda_\alpha)|\psi_{\lambda_\alpha}^+(E|\alpha)\rangle, \\ \langle \chi_f(\beta|\lambda_\beta)|\xi(E)\rangle &= A_{i\lambda_\beta} \langle \chi_f(\beta|\lambda_\beta)|\psi_{\lambda_\beta}^-(E|\beta)\rangle \\ &+ B_{i\lambda_\beta} \langle \chi_f(\beta|\lambda_\beta)|\psi_{\lambda_\beta}^+(E|\beta)\rangle \end{aligned} \quad (74)$$

because of the orthogonality of the internal states of the system. Using Eq. (74), the matrix elements  $A_{i\lambda_\alpha}$ ,  $B_{i\lambda_\alpha}$ ,  $A_{i\lambda_\beta}$ , and  $B_{i\lambda_\beta}$  of channels  $\lambda_\alpha$  and  $\lambda_\beta$  can be calculated by employing two linearly independent final wave packets,  $\chi_f(\alpha|\lambda_\alpha)$ ,  $f = 1, 2$ , in  $\alpha$  arrangement, and two linearly independent final wave packets,  $\chi_f(\beta|\lambda_\beta)$ ,  $f = 1, 2$ , in  $\beta$  arrangement. The  $S$ -matrix can thus be obtained from Eq. (73).

The formulae for solving reactive scattering problems with more than two arrangements are essentially the same as those for the two arrangements case except that more expressions for  $\xi(E|\vec{x})$  (as given in Eqs. (68) and (69)) need to be set up for the additional arrangements. Each arrangement contributes to the sums determining the dimensionality  $(N_\alpha + N_\beta + N_\gamma + \dots) \times (N_\alpha + N_\beta + N_\gamma + \dots)$  of the matrix  $B$ . To solve for the  $S$ -matrix in the multi-arrangement case, one must have  $2(N_\alpha + N_\beta + N_\gamma + \dots) \times (N_\alpha + N_\beta + N_\gamma + \dots)$  linearly independent algebraic equations for the  $A$  and  $B$  matrices. For collision systems involving large numbers of channels, this procedure itself may become a challenge computationally. However, with an absorbing potential or the appropriately chosen attenuating functions,  $d(x_i)$ , to be introduced in the following section, and a slightly larger size of grid, boundary reflections can be avoided. The inhomogeneous time-independent wave packet Schrödinger or Lippmann–Schwinger equation formalism, Eq. (3), or the TIW- $S$ -matrix Kohn variational form of Eq. (3)

$$\begin{aligned} S(\beta n_\beta k_{n_\beta} | \alpha n_\alpha k_{n_\alpha}) &= \frac{i\hbar^2 \sqrt{k_{n_\alpha} k_{n_\beta}}}{m(2\pi)^2 A_\alpha(k_{n_\alpha}) A_\beta^*(k_{n_\beta})} \\ &\times \langle \chi(\beta n_\beta | 0) | G^+(E) | \chi(\alpha n_\alpha | 0) \rangle \end{aligned} \quad (75)$$

for reactive scattering gives a single column of the  $S$ -matrix with one initial wave packet and therefore may be the preferred approach for the most complex problems. The coefficients  $A_\alpha$  and  $A_\beta$  are the Fourier momentum components of the initial wave packet,  $\chi(\alpha n_\alpha | 0)$ , in  $\alpha$  arrange-



ment and final wave packet,  $\chi(\beta n_\beta | 0)$ , in  $\beta$  arrangement at the appropriate wave numbers,  $k_{n_\alpha}$  and  $k_{n_\beta}$ , respectively.

### III. COMPUTATIONAL DETAILS

#### A. Choice of the modified Faber–Chebychev polynomial basis

We must now choose a specific damping factor,  $d(x)$ , which will be used in the modified Faber–Chebychev recursion to generate the damped polynomial basis for expanding the wave function,  $\psi(E|x)$ , or  $\xi(E|x)$ . The resulting damped basis is related to the type used by Mandelshtam and Taylor by a simple transformation.<sup>6</sup> We choose our damping factor to be of a form that tends to preserve continuity and smoothness of the wave function, subject to the constraint that the damped grid Hamiltonian be identical to the original grid Hamiltonian in the interior region. The damped grid Hamiltonian matrix thus constructed will smoothly attenuate the wave function to zero in the boundary region due to the modified Faber–Chebychev recursion's dependence on the  $d(x_i)$  factors. We illustrate the procedure using the solution of Eq. (1),  $\xi(E|x)$ .

(1) We introduce a modified wave function,  $\xi^d(E|x)$ , such that  $\xi^d(E|x)$  is attenuated smoothly to zero near the boundary of the grid (which is equivalent to the effect of an absorbing potential), but in the interior region, it satisfies Eq. (1) with the physical Hamiltonian. To minimize reflections, rapid changes of the derivatives of  $\xi^d(E|x)$  on the grid and at the boundary are avoided. This is achieved by an appropriately damped Hamiltonian, so that in the interior region, the expansion of  $\xi^d(E|x)$  in terms of the  $\eta_n^d$  solves Eq. (1) (or in the case of  $\psi^d(E|x)$ , the ordinary homogeneous time-independent Schrödinger equation) with the physical Hamiltonian.

(2) We expand  $\xi^d(E|x)$  in the polynomial basis,  $\eta_n^d(x)$ , given by Eq. (55) with a choice of expansion coefficients,  $g_n(E_{\text{norm}})$ , given by Eq. (46), which results in a causal-like modified Faber–Chebychev basis expansion of the solution of Eq. (2):

$$\begin{aligned} \xi^d(E) &= -\frac{1}{\sqrt{(\Delta H)^2 - (E - \bar{H})^2}} \sum_n (2 - \delta_{n0}) e^{-in\varphi(E)} \eta_n^d \\ &\equiv \frac{i}{2\pi} G_{\text{damp}}^+(E) \chi(0). \end{aligned} \quad (76)$$

Then as was noted in paper I<sup>4</sup> and in the preceding discussion in Sec. II, the real part of Eq. (76) delivers an approximation to

$$\psi(E) = \delta(E - H) \chi(0) \quad (77)$$

which solves the standard (homogeneous) TISE. We can treat scattering using either Eq. (76), or its real part. The latter has the attractive feature that one can then place the initial packet  $\chi(0)$  on top of the target (that is, the initial packet is non-zero in the region of space associated with the target and projectile being close enough to each other so as to interact).<sup>4</sup> Thus, our approach applies both to solutions of Eq. (1) and of the homogeneous time-independent

Schrödinger equation and the extraction of the scattering information in the two cases is, in general, the same because both kinds of wave functions involve a superposition of a complete set (for any energy  $E$ ) of linearly independent solutions of the Schrödinger equation in the region outside the potential but not yet in the boundary region.

(3) We can achieve (1), by requiring that the damped Hamiltonian, Eq. (53), be such that the basis functions  $\eta_n^d(x)$  generated by Eq. (55) decay to zero smoothly near the boundary. To see how the damping can be made to ensure smooth behavior, we examine Eq. (55) with a real space-dependent damping,  $d(x)$ , applied to the Hamiltonian. For a weak spatial dependence of the damping function,  $d(x)$ ,  $[H, d] \approx 0$  and it follows that

$$H_{\text{damp}} = \sqrt{d(x)} \left[ -\frac{\hbar^2}{2m} \frac{d^2}{dx^2} + V(x) \right] \sqrt{d(x)} \approx d(x)H, \quad (78)$$

and therefore

$$\eta_n^d(x) \approx (d(x))^n \eta_n(x), \quad (79)$$

where the  $\eta_n(x)$  are the basis functions generated by Faber–Chebychev recursion with an undamped Hamiltonian,  $H$ . This indicates that the damped basis functions,  $\eta_n^d(x)$ , decay smoothly to zero near the boundary of the grid if the real space-dependent damping,  $d$ , decreases from one to a value between zero and one, in a small attenuating region including the boundary of the grid. This also implies that the smoothness of the  $\eta_n^d(x)$  and of  $\xi(E|x)$  is related to the smoothness of  $d(x)$ . The form of the space-dependent damping  $d(x)$  chosen for the present study is based on the distributed approximating functional<sup>21</sup> and will be given in Section IV.

#### B. Smoothed Green's operator and Dirac delta function

As noted by Mandelshtam and Taylor,<sup>6</sup> and by Huang *et al.* in a different context,<sup>9</sup> to accelerate further the rate of the convergence of the expansions, of the real and imaginary parts of Eq. (76), a smoothed Green's or delta function can be implemented. Since the expansion for the principal value Green's function  $G^P(E)$  and Dirac delta function,  $\delta(E - H)$ , in Eq. (76) can be viewed as a Fourier series expansion with the variable  $\varphi(E)$ , one can use a well-known local smoothing technique<sup>22</sup> over energy  $E$  to accelerate the Fourier series expansions of  $G^P(E)$  and  $\delta(E - H)$ . There are many possible ways to do the smoothing, and in earlier work, we have used Lanczos'  $\sigma$ -smoothing<sup>22</sup> to accelerate the conformal mapping in the Faber polynomial expansion.<sup>9</sup> In this paper, we use a distributed approximating functional or DAF-based smoothing function,<sup>21</sup>  $\delta_{M_s}(\varphi(E))$ , given by

$$\begin{aligned} \delta_{M_s}(\varphi(E)) &= \frac{1}{\sigma_s} \exp\left(-\frac{\varphi(E)^2}{2\sigma_s^2}\right) \sum_{n=0}^{M_s} \\ &\quad \times \left(-\frac{1}{4}\right)^n (2\pi n!)^{-1/2} H_{2n}\left(\frac{\varphi(E)}{\sqrt{2}\sigma_s}\right), \end{aligned} \quad (80)$$

and obtain the expansion for the smoothed and damped wave function,  $\bar{\xi}^d(E|x)$ ,

$$\xi^{-d}(E|x) = \frac{i}{2\pi} \int d\varphi'(E') \delta_{M_s}(\varphi'(E') - \varphi(E)) G_{\text{damp}}^+(E') \chi(0), \quad (81)$$

which corresponds to an average over energy. The dependence of  $G_{\text{damp}}^+(E')$  on  $\varphi'(E')$ , along with a change of integration variable from  $d\varphi'(E')$  to  $d[\varphi'(E') - \varphi(E)]$  results in a Fourier transform of  $\delta_{M_s}$ , multiplied by  $\exp(-in\varphi(E))$ , and the result is

$$\bar{\xi}^d = \frac{1}{2\pi \sqrt{(\Delta H)^2 - (E - \bar{H})^2}} \sum_n (2 - \delta_{n0}) e^{-in\varphi(E)} \bar{\delta}_{M_s}(n) \eta_n^d. \quad (82)$$

The smoothed and damped real part of  $\bar{\xi}^d$ ,  $\bar{\psi}^d(E)$ , is given by

$$\bar{\psi}^d(E|x) = \frac{1}{\pi \sqrt{(\Delta H)^2 - (E - \bar{H})^2}} \sum_n (2 - \delta_{n0}) \times \cos[n\varphi(E)] \bar{\delta}_{M_s}(n) \eta_n^d(x). \quad (83)$$

Here,  $\bar{\delta}_{M_s}(n)$  is the Fourier transform of  $\delta_{M_s}(\varphi(E))$ ,<sup>23</sup>

$$\bar{\delta}_{M_s}(n) = \sum_{m=0}^{M_s} \frac{\left(\frac{1}{2} \sigma_s^2 n^2\right)^m}{m!} e^{-\sigma_s^2 n^2/2}. \quad (84)$$

In the limit of  $M_s \rightarrow \infty$ , the DAF function,  $\delta_{M_s}(\varphi(E))$ , equals the Dirac  $\delta$  function and  $\bar{\delta}_{M_s}(n) \rightarrow 1$ . For a finite  $M_s$ , the DAF function,  $\delta_{M_s}(\varphi(E))$ , is strongly peaked at zero and the Green's function  $G(E)$  is locally smoothed. However, the exponential decay of the function  $\bar{\delta}_{M_s}(n)$  for  $n > 1/\sigma_s$  truncates the Fourier series expansion, Eq. (82), effectively and results in an accelerated rate of convergence.

#### IV. EXAMPLE CALCULATIONS AND DISCUSSION

We have considered three types of calculations. These are (1) an initial wave packet which sits outside the interaction region and the parameters are such that there is no reflection at the end of the grid, (2) an initial wave packet which sits outside the interaction region and the parameters are such that there is some reflection back into the analysis region, (3) an initial wave packet which sits on top of the interaction. In the second and third cases, the damped and smoothed wave functions,  $\bar{\xi}^d(E)$ , over a range of energies,  $E$ , can be obtained from Eq. (82) by building up the space-dependent damped Faber–Chebychev basis vectors,  $\eta_n^d$ , using the recursion (55). One then projects  $\bar{\xi}^d(E)$  on to a number of final wave packets,  $\chi_f$ , located just outside the potential in the various arrangement regions, and calculates the elements of matrices  $A$  and  $B$  using Eq. (74). The number of final wave packets is twice the number of open channels in the arrangement. Finally, the full  $S$ -matrix as a func-

tion of energy can be obtained by repeating the above procedure for a number of initial wave packets, which is equal to the number of open channels of all arrangements, and using Eq. (73).

The damping function,  $d(x)$ , is the key to constructing the damped Faber–Chebychev basis vectors,  $\eta_n^d$ , and attenuating the wave function  $\bar{\xi}^d(E)$  so that the effects of reflection can be minimized. The attenuating region is chosen not to overlap the interaction potential, the initial and final wave packets. To avoid reflection in region of attenuation, the function  $d$  should not decrease too abruptly. One wants, however, the region of attenuation to be as small as possible. These opposing constraints must be balanced and we have found that reasonable results can be obtained with an attenuating factor  $d$  constructed using a functional form related to the DAF.<sup>21</sup> We term the function the ‘‘conjugated DAF function’’ (related to the Fourier transform of the standard DAF). In one dimension, the function is given by

$$d(x) = \sum_{m=0}^{M_d} \frac{\left[\frac{1}{2}(\sigma_d x)^p\right]^m}{m!} e^{-(\sigma_d x)^p/2}, \quad (85)$$

where the power  $p$  is used to control the fall off of  $d(x)$  in the attenuation region. With  $p=2$ , the conjugated DAF function is exactly the Fourier transform of the DAF,<sup>21,23</sup> which is the same quantity used to smooth the Green and spectral density operators. The  $d(x)$  given in Eq. (85) delivers a smooth decay of the  $\eta_n^d$  at the boundary. The parameters of  $d(x)$  are chosen so that it does not decay to zero at the end of the boundary, but rather to a value of 0.5. As a result, the wave function  $\bar{\xi}_i^d(E)$  decays smoothly to a small value in the attenuating region and reflection is reduced significantly.

We have applied this scaling of the Hamiltonian, the space-dependent damped Faber–Chebychev basis vectors, the smoothed Green's function and delta function expressions, and the final state analysis, to collinear H+H<sub>2</sub> reactive scattering. The LSTH potential<sup>24</sup> and reactant arrangement Jacobi coordinates ( $x, y$ ) are used in the calculation. The DAF method<sup>21</sup> is used to represent the wave function and kinetic energy operator on the grid, which has four grid points per de Broglie wavelength at the energy  $E = 1.4$  eV. The attenuation region starts at 6.8 a.u. and extends out to 7.8 a.u. The three parameters determining  $d(x)$  in Eq. (85) are:  $p = 2.0$ ,  $\sigma_d = 10.0/6.8$  and  $M_d = 70$ . The ratio 10.0/6.8 yields a numerical value for  $\sigma_d$  that causes the damping to begin at about  $x = 6.8$ . The value of the damping function,  $d(x)$ , at the end of the boundary is 0.5. The parameters of the smoothing DAF for the Green and delta function operators,  $\delta_{M_s}(\varphi(E))$ , in Eq. (80) are:  $\sigma_s = 1.0/220.0$ ,  $M_s = 10$ . The ratio 1.0/220.0 results in a numerical value of  $\sigma_s$  that causes the smoothing to begin after about 220 terms in the sum. The results are found to be very stable and to converge without difficulty. The calculated transition probabilities at 1300 Faber–Chebychev iterations are given in Tables I, II, and III for the Green's function and initial packet outside the target. In Table IV, similar results are given for the spectral density or delta function, with the initial packet on top of the

TABLE I. Reactive and inelastic transition probabilities of collinear H+H<sub>2</sub> at  $E=0.5$  eV calculated using Green's function operator.

| Arrangement | State | $\alpha$<br>0                                      | $\beta$<br>0                                       |
|-------------|-------|--|--|
| $\alpha$    | 0     | 0.917<br>(0.917) <sup>a</sup>                      | $8.33 \times 10^{-2}$<br>( $8.30 \times 10^{-2}$ ) |
| $\beta$     | 0     | $8.35 \times 10^{-2}$<br>( $8.30 \times 10^{-2}$ ) | 0.919<br>(0.917)                                   |

<sup>a</sup>Data given in parentheses are calculated in terms of  $S$ -matrix Kohn variational method.

target. The results are all compared to those obtained with the  $S$ -matrix Kohn variational method.<sup>25</sup> Agreement is to within 1.0% for most of the transitions. We found that the spectral density operator method converged more quickly than the Green's function approach (the results are converged after about 1000 Faber-Chebyshev iterations).<sup>4,9</sup> This probably reflects the fact that the packet already is on top of the target so one does not have to "propagate" it from outside into the target. Furthermore, we find that the present version of the delta function approach is considerably less sensitive to the details of the initial packet than was the earlier version of the approach (which did not employ the damped Hamiltonian and concomitant damped Faber-Chebyshev basis vectors<sup>4</sup>). It is also found in both forms of this method that results at some energies converged more quickly than others. Thus, fewer numbers of polynomials are needed to obtain converged results at some energies than others.

The disadvantage of allowing reflections from the boundary is that one must solve linear algebraic equations for the full  $S$ -matrix in order to obtain transition probabilities from any one state. If there are a very large number of states accessible at the range of energies of interest, then this can become a computationally demanding part of the calculation. In that case, it may be better to do the calculation in a rela-

TABLE II. Transition probabilities of collinear H+H<sub>2</sub> at  $E=1.1$  eV using Green's function.

| Inelastic         | $\alpha \rightarrow \alpha$ |                      | $\beta \rightarrow \beta$  |         |
|-------------------|-----------------------------|----------------------|----------------------------|---------|
| 0 $\rightarrow$ 0 | 0.170                       | (0.172) <sup>a</sup> | 0.170                      | (0.172) |
| 0 $\rightarrow$ 1 | 0.154                       | (0.153)              | 0.150                      | (0.153) |
| 1 $\rightarrow$ 0 | 0.152                       | (0.153)              | 0.150                      | (0.153) |
| 1 $\rightarrow$ 1 | 0.122                       | (0.123)              | 0.123                      | (0.123) |
| Reactive          | $\alpha \rightarrow \beta$  |                      | $\beta \rightarrow \alpha$ |         |
| 0 $\rightarrow$ 0 | 0.295                       | (0.296)              | 0.298                      | (0.296) |
| 0 $\rightarrow$ 1 | 0.383                       | (0.380)              | 0.381                      | (0.380) |
| 1 $\rightarrow$ 0 | 0.380                       | (0.380)              | 0.380                      | (0.380) |
| 1 $\rightarrow$ 1 | 0.341                       | (0.344)              | 0.340                      | (0.344) |

<sup>a</sup>Data given in parentheses are calculated in terms of  $S$ -matrix Kohn Variational principle.

TABLE III. Transition probabilities of collinear H+H<sub>2</sub> at  $E=1.4$  eV using the Green's function.

| Inelastic         | $\alpha \rightarrow \alpha$ |                           | $\beta \rightarrow \beta$  |                           |
|-------------------|-----------------------------|---------------------------|----------------------------|---------------------------|
| 0 $\rightarrow$ 0 | 0.301                       | (0.300) <sup>a</sup>      | 0.302                      | (0.300)                   |
| 0 $\rightarrow$ 1 | 0.222                       | (0.220)                   | 0.223                      | (0.220)                   |
| 0 $\rightarrow$ 2 | $8.98 \times 10^{-2}$       | ( $8.91 \times 10^{-2}$ ) | $9.10 \times 10^{-2}$      | ( $8.91 \times 10^{-2}$ ) |
| 1 $\rightarrow$ 0 | 0.220                       | (0.220)                   | 0.224                      | (0.220)                   |
| 1 $\rightarrow$ 1 | $8.94 \times 10^{-2}$       | ( $8.74 \times 10^{-2}$ ) | $8.85 \times 10^{-2}$      | ( $8.74 \times 10^{-2}$ ) |
| 1 $\rightarrow$ 2 | $4.01 \times 10^{-2}$       | ( $3.86 \times 10^{-2}$ ) | $4.44 \times 10^{-2}$      | ( $3.86 \times 10^{-2}$ ) |
| 2 $\rightarrow$ 0 | $9.07 \times 10^{-2}$       | ( $8.91 \times 10^{-2}$ ) | $9.36 \times 10^{-2}$      | ( $8.91 \times 10^{-2}$ ) |
| 2 $\rightarrow$ 1 | $4.07 \times 10^{-2}$       | ( $3.86 \times 10^{-2}$ ) | $3.71 \times 10^{-2}$      | ( $3.86 \times 10^{-2}$ ) |
| 2 $\rightarrow$ 2 | 0.153                       | (0.157)                   | 0.151                      | (0.157)                   |
| Reactive          | $\alpha \rightarrow \beta$  |                           | $\beta \rightarrow \alpha$ |                           |
| 0 $\rightarrow$ 0 | $5.89 \times 10^{-2}$       | ( $5.96 \times 10^{-2}$ ) | $5.94 \times 10^{-2}$      | ( $5.96 \times 10^{-2}$ ) |
| 0 $\rightarrow$ 1 | 0.228                       | (0.224)                   | 0.221                      | (0.224)                   |
| 0 $\rightarrow$ 2 | 0.104                       | (0.107)                   | 0.102                      | (0.107)                   |
| 1 $\rightarrow$ 0 | 0.226                       | (0.224)                   | 0.225                      | (0.224)                   |
| 1 $\rightarrow$ 1 | 0.307                       | (0.305)                   | 0.306                      | (0.305)                   |
| 1 $\rightarrow$ 2 | 0.120                       | (0.126)                   | 0.120                      | (0.126)                   |
| 2 $\rightarrow$ 0 | 0.103                       | (0.107)                   | 0.101                      | (0.107)                   |
| 2 $\rightarrow$ 1 | 0.121                       | (0.126)                   | 0.116                      | (0.126)                   |
| 2 $\rightarrow$ 2 | 0.503                       | (0.482)                   | 0.502                      | (0.482)                   |

<sup>a</sup>Data given in parentheses are calculated in terms of  $S$ -matrix Kohn variational method.

TABLE IV. Transition probabilities of collinear H+H<sub>2</sub> at  $E=1.4$  eV calculated using spectral density operator.

| Inelastic         | $\alpha \rightarrow \alpha$ |                           | $\beta \rightarrow \beta$  |                           |
|-------------------|-----------------------------|---------------------------|----------------------------|---------------------------|
| 0 $\rightarrow$ 0 | 0.295                       | (0.300)                   | 0.299                      | (0.300)                   |
| 0 $\rightarrow$ 1 | 0.222                       | (0.220)                   | 0.225                      | (0.220)                   |
| 0 $\rightarrow$ 2 | $8.96 \times 10^{-2}$       | ( $8.91 \times 10^{-2}$ ) | $9.14 \times 10^{-2}$      | ( $8.91 \times 10^{-2}$ ) |
| 1 $\rightarrow$ 0 | 0.221                       | (0.220)                   | 0.225                      | (0.220)                   |
| 1 $\rightarrow$ 1 | $8.85 \times 10^{-2}$       | ( $8.74 \times 10^{-2}$ ) | $8.83 \times 10^{-2}$      | ( $8.74 \times 10^{-2}$ ) |
| 1 $\rightarrow$ 2 | $3.96 \times 10^{-2}$       | ( $3.86 \times 10^{-2}$ ) | $4.33 \times 10^{-2}$      | ( $3.86 \times 10^{-2}$ ) |
| 2 $\rightarrow$ 0 | $9.20 \times 10^{-2}$       | ( $8.91 \times 10^{-2}$ ) | $9.45 \times 10^{-2}$      | ( $8.91 \times 10^{-2}$ ) |
| 2 $\rightarrow$ 1 | $4.00 \times 10^{-2}$       | ( $3.86 \times 10^{-2}$ ) | $4.64 \times 10^{-2}$      | ( $3.86 \times 10^{-2}$ ) |
| 2 $\rightarrow$ 2 | 0.162                       | (0.157)                   | 0.160                      | (0.157)                   |
| Reactive          | $\alpha \rightarrow \beta$  |                           | $\beta \rightarrow \alpha$ |                           |
| 0 $\rightarrow$ 0 | $6.04 \times 10^{-2}$       | ( $5.96 \times 10^{-2}$ ) | $6.09 \times 10^{-2}$      | ( $5.96 \times 10^{-2}$ ) |
| 0 $\rightarrow$ 1 | 0.225                       | (0.224)                   | 0.220                      | (0.224)                   |
| 0 $\rightarrow$ 2 | 0.106                       | (0.107)                   | 0.104                      | (0.107)                   |
| 1 $\rightarrow$ 0 | 0.225                       | (0.224)                   | 0.222                      | (0.224)                   |
| 1 $\rightarrow$ 1 | 0.305                       | (0.305)                   | 0.304                      | (0.305)                   |
| 1 $\rightarrow$ 2 | 0.120                       | (0.126)                   | 0.122                      | (0.126)                   |
| 2 $\rightarrow$ 0 | 0.109                       | (0.107)                   | 0.107                      | (0.107)                   |
| 2 $\rightarrow$ 1 | 0.124                       | (0.126)                   | 0.128                      | (0.126)                   |
| 2 $\rightarrow$ 2 | 0.473                       | (0.482)                   | 0.471                      | (0.482)                   |

<sup>a</sup>Data given in parentheses are calculated in terms of  $S$ -matrix Kohn Variational principle.

TABLE V. Transition probabilities of collinear H+H<sub>2</sub> calculated using the TIW-S-matrix Kohn variational equation.

| Transition | Energy |                       | Inelastic               |                       | Reactive                |  |
|------------|--------|-----------------------|-------------------------|-----------------------|-------------------------|--|
|            | (eV)   |                       |                         |                       |                         |  |
| 0→0        | 0.5    | 0.871                 | (0.917)                 | $8.28 \times 10^{-2}$ | $(8.30 \times 10^{-2})$ |  |
|            | 1.1    | 0.177                 | (0.172)                 | 0.297                 | (0.296)                 |  |
|            | 1.4    | 0.288                 | (0.300)                 | $6.30 \times 10^{-2}$ | $(5.96 \times 10^{-2})$ |  |
| 0→1        | 1.1    | 0.152                 | (0.153)                 | 0.379                 | (0.380)                 |  |
|            | 1.4    | 0.226                 | (0.220)                 | 0.228                 | (0.224)                 |  |
| 0→2        | 1.4    | $8.80 \times 10^{-2}$ | $(8.91 \times 10^{-2})$ | 0.104                 | (0.107)                 |  |

<sup>a</sup>Data given in parentheses are calculated in terms of S-matrix Kohn variational method.

tively larger region to avoid boundary reflections, and use the expressions, Eqs. (3) and (75), we presented earlier for the causal solution.<sup>2,9</sup> In that case, one can completely avoid having to solve large systems of algebraic equations and the calculation reduces to applying the highly banded, sparse Hamiltonian matrix to a vector. To reduce boundary reflections to a small, negligible amount, we enlarged the attenuation region (which starts at 8.0 a.u.) to 3.0 a.u. The shift of the region allows for the initial wave packet to be placed outside the potential. The parameters for  $d(x)$  are the same except  $\sigma_d=10.0/9.5$  is chosen, so the damping region now begins at about  $x=9.5$ . *Smoothing was not used in this case.* The results for a single column of the S-matrix, Eq. (75), calculated at 1500 Faber–Chebychev iterations, are given in Table V. Agreement is to within 5.0%.

## V. CONCLUSIONS

We have presented a detailed analysis of how one can obtain scattering as a continuous function of energy even though the Hamiltonian is approximated by a finite discrete matrix (resulting from enclosing the system artificially in a finite region and discretizing the coordinates). Such solutions are constructed for both the standard homogeneous time-independent Schrödinger equation and the inhomogeneous time-independent wave packet Schrödinger equation. An important additional result is an analytical expression for the error incurred in a finite truncation of the expansion of these solutions. Effects due to reflections off the boundaries are brought under control by introducing a spatially damped real Hamiltonian, which agrees with the ordinary one except in the boundary region, as done by Mandelshtam and Taylor.<sup>6</sup> In the boundary region, the damped Hamiltonian is attenuated smoothly. This leads naturally to a space-dependent damped modified Faber–Chebychev polynomial basis, and expressions have been developed for corresponding approximate solutions to the inhomogeneous time-independent wave packet Schrödinger and homogeneous time-independent Schrödinger equations. This makes it possible to use smaller regions in which to carry out scattering calculations, thereby improving the efficiency. In addition, new analytical expressions were derived for the truncation error. These should be

extremely useful in determining the optimal points at which to carry out the evaluation of the scattering information.

We also introduced a “conjugated DAF function” as a particular choice of damping function which smoothly attenuates the solutions of Eqs. (1) and (2) to zero at the boundary. A method for accelerating the rate of the convergence of the polynomial expansion is also introduced, based on locally averaging (smoothing) the operators in the energy space. This convergence acceleration method is applied both to the modified Faber–Chebychev expansion of the principle-value Green’s function and to the spectral density operator acting on initial wave packets. Further, the expressions can also be evaluated in terms of the eigenvalues and eigenstates of the damped Hamiltonian, and they yield accurate results for energies both at and away from the eigenvalues. We will be reporting applications to other systems (including full three dimensional reactive scattering) in later communications.

## ACKNOWLEDGMENTS

Y.H. is supported in part under National Science Foundation Grants Nos. CHE94-03416 and is a NSF Advanced Scientific Computing Fellow under Grant No. ASC93-10235. S.I. is supported in part under R. A. Welch Foundation Grant No. E-0608. D.J.K. is supported in part under R. A. Welch Foundation Grant No. E-0608. The Ames Laboratory is operated for the Department of Energy by Iowa State University under Contract No. 2-7405-ENG82.

- <sup>1</sup>D.J. Kouri, M. Arnold, and D.K. Hoffman, Chem. Phys. Lett. **203**, 166 (1993).
- <sup>2</sup>Y. Huang, W. Zhu, D.J. Kouri, and D.K. Hoffman, Chem. Phys. Lett. **206**, 96 (1993); **213**, 209 (1993).
- <sup>3</sup>W. Zhu, Y. Huang, D.J. Kouri, M. Arnold, and D.K. Hoffman, Phys. Rev. Lett. **72**, 1310 (1994).
- <sup>4</sup>D.K. Hoffman, Y. Huang, W. Zhu, and D.J. Kouri, J. Chem. Phys. **101**, 1242 (1994).
- <sup>5</sup>D.J. Kouri, Y. Huang, W. Zhu, and D.K. Hoffman, J. Chem. Phys. **100**, 3662 (1994).
- <sup>6</sup>V.A. Mandelshtam and H.S. Taylor, J. Chem. Phys. **102**, 7390 (1995); **103**, 2903 (1995).
- <sup>7</sup>H.W. Jang and J.C. Light, J. Chem. Phys. **102**, 3262 (1995).
- <sup>8</sup>Y. Huang, D.J. Kouri, and D.K. Hoffman, Chem. Phys. Lett. **225**, 37 (1994).
- <sup>9</sup>Y. Huang, D.J. Kouri, and D.K. Hoffman, J. Chem. Phys. **101**, 10493 (1994).
- <sup>10</sup>H. Tal-Ezer and R. Kosloff, J. Chem. Phys. **81**, 3967 (1984).
- <sup>11</sup>R. Kosloff, J. Phys. Chem. **92**, 2087 (1988).
- <sup>12</sup>I.S. Gradshteyn and I.M. Ryzhik, *Table of Integrals, Series, and Products* (Academic, New York, 1980).
- <sup>13</sup>D.J. Kouri, W. Zhu, G.A. Parker, and D.K. Hoffman, Chem. Phys. Lett. **238**, 395 (1995).
- <sup>14</sup>G.A. Parker, W. Zhu, Y. Huang, D.J. Kouri, and D.K. Hoffman, Comp. Phys. Commun. (in press).
- <sup>15</sup>G. Arfken, *Mathematical Methods for Physicists*, 3rd ed. (Academic, New York, 1985), pp. 736–739.
- <sup>16</sup>D. Neuhauser and M. Baer, J. Chem. Phys. **90**, 4351 (1989).
- <sup>17</sup>D. Neuhauser, M. Baer, R.S. Judson, and D.J. Kouri, J. Chem. Phys. **90**, 5882 (1989); **93**, 312 (1990).
- <sup>18</sup>M. Reed and B. Simon, *Scattering Theory* (Academic, New York, 1979), Vol. III; M.L. Goldberger and K.M. Watson, *Collision Theory* (Krieger, New York, 1975).

- <sup>19</sup>T. Seideman and W.H. Miller, *J. Chem. Phys.* **96**, 4412 (1992).
- <sup>20</sup>A. Vibok and G.G. Balint-Kurti, *J. Chem. Phys.* **96**, 7615 (1992).
- <sup>21</sup>D.K. Hoffman, N. Nayar, O.A. Sharafeddin, and D.J. Kouri, *J. Phys. Chem.* **95**, 8299 (1991).
- <sup>22</sup>C. Lanczos, *Discourse on Fourier Series* (Hafner, New York, 1966).
- <sup>23</sup>Y. Huang, D.J. Kouri, M. Arnold, T.L. Marchioro II, and D.K. Hoffman, *Comp. Phys. Commun.* **80**, 1 (1994).
- <sup>24</sup>B. Liu, *J. Chem. Phys.* **58**, 1925 (1973); P. Siegbahn and B. Liu, *ibid.* **68**, 2457 (1978); D.G. Truhlar and C.J. Horowitz, *ibid.* **68**, 2466 (1978); **71**, 1514(E) (1979).
- <sup>25</sup>G.C. Groenenboom and D.T. Colbert, *J. Chem. Phys.* **99**, 9681 (1993).